

# PARALLEL TRACKING-BASED MODELING OF GAS SCATTERING AND LOSS DISTRIBUTIONS IN ELECTRON STORAGE RINGS\*

M. Borland, ANL, Argonne, IL, USA

## Abstract

Estimation of gas scattering lifetimes in storage rings is typically done using a simple approach that can readily be performed by hand. A more sophisticated approach uses linear mapping of the angular dynamic acceptance around the ring and allows including variation of gas pressure and composition [1]. However, neither approach is appropriate for highly nonlinear lattices, in which the angular acceptance does not map according to the linear optics. Further, these approaches provide no detailed information about the location of losses. To address these limitations, a tracking-based approach was implemented in the program Pelegant [2–4]. We describe the implementation and performance of this method, as well as application to the Advanced Photon Source Upgrade.

## INTRODUCTION

In third-generation storage ring light sources, the lifetime is typically dominated by Touschek scattering, so an approximate knowledge of the gas-scattering lifetime is sufficient. Calculation of gas-scattering lifetime is thus often considered a closed subject needing little advancement beyond handbook-level formulae involving the minimum physical aperture and momentum acceptance (see, e.g., [5]). However, for fourth-generation storage ring light sources, the nonlinear dynamics is more challenging and gas scattering deserves a closer look. In [1], we described how to compute the gas scattering lifetime from the dynamic acceptance (DA) and local momentum acceptance (LMA) [6, 7], along with species-specific gas pressure distributions. The DA was mapped around the ring using the linear lattice functions to provide an  $s$ -dependent angular acceptance, which was then used with the  $s$ -dependent pressure data to compute the local out-scattering rate and hence the elastic-scattering lifetime. The LMA was used more directly with the  $s$ -dependent pressure data to compute the local out-scattering rate for inelastic scattering.

While this improves upon simpler approaches, mapping the DA using the linear lattice functions is not reliable in lattices with strong nonlinearities. In addition, this method provides no information on where out-scattered particles are lost. The present work addresses these issues through development of a tracking-based approach that reflects the full complexity of the nonlinear dynamics and  $s$ -dependent, multi-species gas pressure profiles.

\* Work supported by the U.S. Department of Energy, Office of Science, Office of Basic Energy Sciences, under Contract No. DE-AC02-06CH11357.

The gas scattering lifetime is computed using [1]

$$\frac{1}{\tau} = \frac{c}{L} \sum_{g=1}^G \sum_{a=1}^{C_g} \int_0^L \sigma_{g,a}(s) S_{g,a} n_g(s) ds, \quad (1)$$

where  $L$  is the length of a periodic section of the ring,  $G$  is the number of molecular gas constituents,  $C_g$  is the number of atomic components of gas  $g$ ,  $\sigma_{g,a}(s)$  is the out-scattering cross section for atomic component  $a$  of gas  $g$  at location  $s$ ,  $S_{g,a}$  is the number of atoms of type  $a$  in a molecule of gas  $g$ , and  $n_g(s)$  is the number density of gas  $g$  at location  $s$ .

In order to evaluate this equation, we use tracking to determine the  $s$ -dependent out-scattering cross section,

$$\sigma_{g,a}(s) = \int_{q_1(s)}^{q_2(s)} \frac{d\sigma_{g,a}}{dq} dq, \quad (2)$$

where  $q$  is the scattering coordinate,  $q_1$  is the maximum surviving value of  $q$ , and  $q_2$  is the physically-limiting value of  $q$ . For elastic scattering,  $q$  is the scattering angle  $\theta$ , while for inelastic scattering,  $q$  is the change in fractional momentum deviation  $\delta$ .

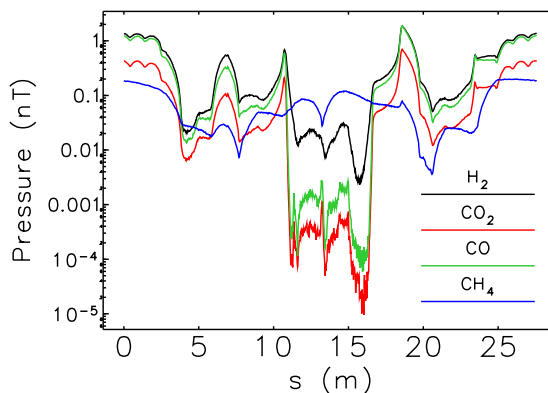


Figure 1: Simulated pressure profiles for one sector of APS-U. Data courtesy J. A. Carter (APS).

## ELASTIC SCATTERING LIFETIME

Elastic scattering from atomic nuclei is described by the Rutherford cross section [8]

$$\frac{d\sigma_{g,a}}{d\Omega} = \frac{Z_{g,a}^2 r_e^2}{4\gamma^2} \frac{1}{\sin^4 \frac{\theta}{2}}, \quad (3)$$

with  $\theta$  the scattering angle,  $Z_{g,a}$  the atomic number,  $r_e$  the classical electron radius, and  $\gamma$  is relativistic factor.

To compute the lifetime, we only need to know the DA boundary  $\theta_a(\phi, s)$ . However, to determine the loss distribution, we need to track particles that are scattered to angles

that exceed  $\theta_a(\phi, s)$ . Hence, rather than perform a DA boundary search, we track a grid of particles distributed over  $(\theta, \phi)$  starting at many  $s$  locations. This is performed in Pelegant using the command `elastic_scattering`.

The algorithm requires the user to specify  $s$  locations at which tracking will start; this can be done using wild-cards to identify locations by name. At each location, Pelegant creates an initial grid of particles uniformly distributed in spherical angles  $(\theta, \phi)$ , with  $\phi \in [0, \pi]$ . The user specifies the minimum  $\theta$ , which should be inside the DA at all  $s$  locations, and the maximum  $\theta$ , which should be greater than  $\sim 4\theta_{\min}$  so that the cross section falls by a factor of more than 100. These limits can optionally be scaled with the local beta functions, while can approximately optimize their values for each location. The code warns the user if any particles on the inner  $\theta$  boundary are lost or if any particles on the outer  $\theta$  boundary survive.

Following scattering, tracking continues until the number of turns specified by the user have been executed. For particles that are lost, the scattering location, scattering angles, loss location, and coordinates at loss are recorded for later analysis.

To determine the elastic scattering lifetime and local loss rates, we need to perform the integral in Eq. (1) using the cross-section in Eq. (3). All the integrals must be discretized, which is straightforward, giving

$$\frac{1}{\tau} \approx \frac{2c}{L} \sum_l L_l \langle G(s)W(s) \rangle_l \sum_{i=0}^{N_\phi-1} \Delta\phi \sum_{j=0}^{N_\theta-1} \Delta\theta \frac{\sin\theta_j}{\sin^4\frac{\theta_j}{2}} T_{i,j,l}, \quad (4)$$

where the index  $l$  is over scattering locations,  $L_l$  is the length of the segment represented by the  $l^{\text{th}}$  scattering location,  $\langle \rangle_l$  represents an average over that segment,  $i$  indexes azimuthal angles  $\phi : [0, \pi]$  spaced by  $\Delta\phi$ , and  $j$  indexes polar angles  $\theta$  spaced by  $\Delta\theta$ . Since we restrict  $\phi : [0, \pi]$ , we need a factor of 2 in front of the expression.  $T_{i,j,l}$  represents whether the particle scattered with angles  $\phi = i\Delta\phi$  and  $\theta_j = j\Delta\theta$  from location  $l$  was lost as determined from tracking; the value is 1 (0) for particles that are lost (not lost).  $G(s)$  is related to the gas properties while  $W(s)$  is a beta-function weighting factor, so that

$$\langle GW \rangle_l = \int_{s_{l,1}}^{s_{l,2}} \frac{ds}{L_l} \sum_{g=1}^{N_g} n_g(s) \sum_{a=1}^{C_g} S_{g,a} \left( \frac{Z_g a r_e}{2\gamma} \right)^2 \sqrt{\frac{\beta_x(s) \beta_y(s)}{\beta_{xl} \beta_{yl}}}, \quad (5)$$

where the integral is over the region  $s : [s_{l,1}, s_{l,2}]$  represented by the  $l^{\text{th}}$  scattering location. These computations are performed with the program `elasticScatteringAnalysis`, which is distributed with `elegant`. Performing these computations with an external program allows using the tracking results with different pressure distributions.

The tracking is embarrassingly parallel and should scale well with appropriate domain decomposition. To avoid expensive load rebalancing, the decomposition ensures that the workload for each of  $C_w$  working cores is about the same. Each working core starts with the same number of

on-axis particles, each of which has a particle ID  $p$  that is unique across all cores. The particle IDs range between 1 and  $N_l N_\theta N_\phi$ , where  $N_l$  is the number of scattering locations. Successive particle IDs  $p$  on a given core are spaced by  $C_w$ , so that the particle IDs are striped across cores. On the first tracking turn, each core decides based on the particle ID value where and by how much to scatter each of its particles. The method of assigning particles to scattering locations and amplitudes ensures that the full scattering grid is explored for each scattering location, but that no core is likely to have particles from only one location or region of  $(\theta, \phi)$  space.

We tested the parallel performance of the algorithm on an APS-U test case. Because of the time-consuming nature of the runs, we performed 50-turn simulations for only 1/10 of the APS-U ring, and did not use fewer than 16 cores. The efficiency exceeds 86% for up to 640 cores, the largest number tested.

## INELASTIC SCATTERING

Simulation of inelastic scattering is similar to simulation of elastic scattering, but simpler. The differential cross-section for atomic number  $Z$  is given by [9, 10]

$$\frac{d\sigma}{dk} = 4\alpha r_e^2 \left\{ \left( \frac{4}{3k} - \frac{4}{3} + k \right) T_1(Z) + \frac{T_2(Z)}{9} \left( \frac{1}{k} - 1 \right) \right\}, \quad (6)$$

where  $k$  is the energy of the emitted photon as a fraction of the electron energy, and the functions  $T_1(Z)$  and  $T_2(Z)$  are described in [10]. The fractional change in energy of the scattered electron is  $u = -k$ . The limiting energy aperture  $k_{\text{ap}}$  is a function of  $s$ .

The relevant nonlinear dynamics result is the negative-side local momentum acceptance (LMA). However, if we wish to determine the distribution of lost particles, we must track particles starting (more or less) at the LMA boundary and beyond. This is particularly relevant for brehmsstrahlung scattering because the cross-section is a weak function of the normalized photon energy  $k$ . One might think that modifying Pelegant's Touschek scattering code [11] would be the most expedient approach, however, the scattering cross-section is much different, which significantly changes the simulation approach.

As in the case of elastic scattering, here we track many particles scattered from many locations. Instead of a 2-d grid of scattering coordinates  $(\theta, \phi)$ , we have a single scattering amplitude  $k$ . Since the scattering cross-section is roughly proportional to  $1/k$ , we spaced the scattering amplitudes uniformly in  $1/k$ . As in the case of Touschek scattering, the range of  $k$  values can be narrowed down by using the previously-determined LMA, which gives  $k_{\min}(s)$ .

Because only a 1-d grid is needed, these simulations are much less demanding than those for elastic scattering. The efficiency is above 88% for up to 640 cores.

To determine the inelastic scattering lifetime and local loss rates, we need to perform the integral in Eq. (1) using the cross-section in Eq. (6) with the  $s$ -dependent limits on

the integral determined by the tracking results. The discretization is straightforward, and we omit it here for lack of space. The analysis is performed using an external program called `inelasticScatteringAnalysis`, which is distributed with `elegant`.

## RESULTS FOR APS-U LATTICE

The methods described above were applied to the APS-U lattice [12], which is a 6-GeV, hybrid multi-bend achromat [13] with reverse bends [14, 15]. For elastic scattering, we used  $N_\phi = N_\theta = 31$ , 112 scattering locations in each of 40 sectors, and 504 Broadwell cores per job. Scattering locations were at the exit of every dipole segment, quadrupole, sextupole, and beam position monitor. For inelastic scattering, we used  $N_k = 50$ , 34 scattering locations per sector, and 1024 lower-performance Knights-Landing cores per job. Scattering locations were at the exit of every dipole and quadrupole. Based on experience, we tracked for 500 turns for elastic scattering but 1500 for inelastic scattering. All simulations included rf cavities, multipole errors, lattice errors and corrections, physical apertures, and radiation effects. The gas-pressure distribution is based the most recent APS-U vacuum system design [16], which is similar to that described in [1]. Figure 1 shows the  $s$ -dependent pressure profiles.

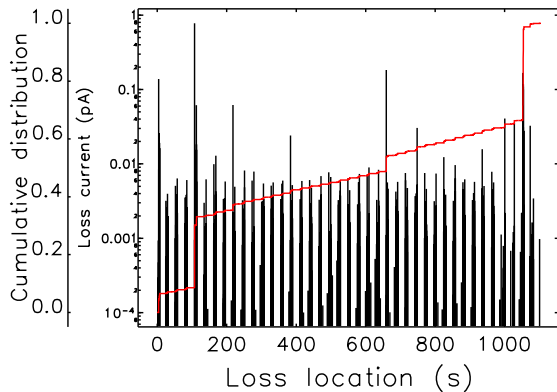


Figure 2: Distribution of elastic scattering losses for worst-case loss rate for APS-U. Highest losses are seen at the vertical collimators and the smallest-aperture insertion device. The red curve is the cumulative distribution integrated over the loss location.

Figures 2 and 3 show the worst-case loss rates from 100 post-commissioning ensembles [17, 18]. The pressure distributions used for these calculations are for 200 mA stored beam with 1000 Ah conditioning [16]. The locations of the highest losses correspond in reasonable ways to the locations of small apertures, such as insertion devices and collimators. However, there are also significant losses distributed around the ring, which is particularly evident in the inelastic scattering results. Figure 4 shows the cumulative distribution of the lifetimes. We see that the elastic gas scattering lifetimes exhibit much more variation, which seems plausible given that

the inelastic gas scattering lifetime depends logarithmically on the momentum acceptance [5].

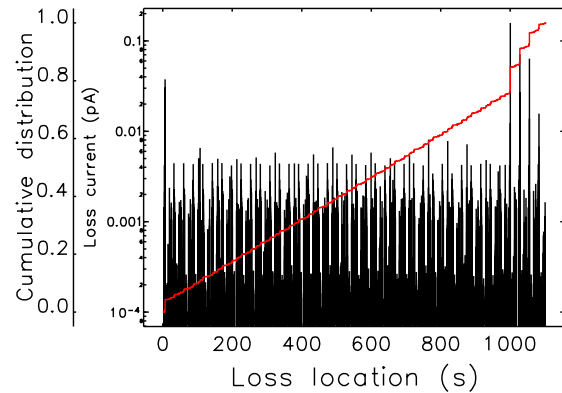


Figure 3: Distribution of inelastic scattering losses for worst-case loss rate for APS-U. Highest losses are seen at the five horizontal collimators.

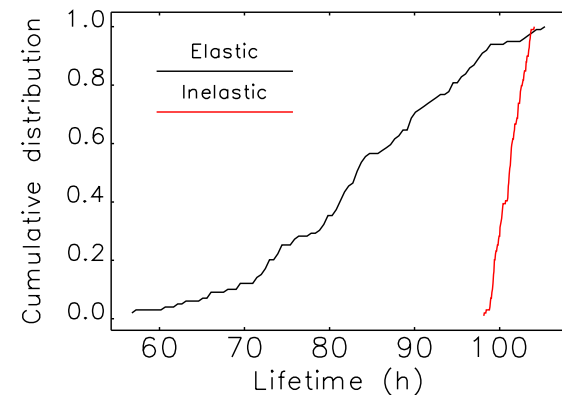


Figure 4: Cumulative distributions of the elastic and inelastic gas scattering lifetimes for APS-U. The median total gas scattering lifetime is about 45 hours.

## CONCLUSIONS

Tracking-based methods for simulating the elastic and inelastic gas scattering lifetimes and loss distributions have been implemented in the parallel code `Pelegant`. Parallel scaling is excellent up to 640 cores, the largest number studied. Application to the APS upgrade lattice gives not only lifetime distributions, but also the spatial distribution of losses around the ring. The latter are used as input into radiation shielding analysis.

## ACKNOWLEDGMENTS

This work used the Blues and Bebop clusters at Argonne National Laboratory. Jason Carter (APS) provided gas pressure data.

## REFERENCES

- [1] M. Borland, J. Carter, H. Cease, and B. Stillwell, "Simulation of gas-scattering lifetime using position- and species-dependent pressure and aperture profiles," in *Proc. IPAC 2015*, p. 546, 2015.
- [2] M. Borland, "elegant: A Flexible SDDS-Compliant Code for Accelerator Simulation," Tech. Rep. ANL/APS LS-287, Advanced Photon Source, September 2000.
- [3] Y. Wang and M. Borland, "Pelegant: A Parallel Accelerator Simulation Code for Electron Generation and Tracking," *AIP Conf. Proc.*, vol. 877, p. 241, 2006.
- [4] Y. Wang, M. Borland, H. Shang, and R. Soliday, "Recent progress on parallel elegant," in *Proc. ICAP 2009*, pp. 355–357, 2009.
- [5] J. Le Duff, "Current and current density limitations in existing electron storage rings," *NIM A*, vol. 239, 1985.
- [6] C. Steier, D. Robin, L. Nadolski, W. Decking, Y. Wu, and J. Laskar, "Measuring and optimizing the momentum aperture in a particle accelerator," *Phys. Rev. E*, vol. 65, p. 056506, May 2002.
- [7] M. Belgroune, P. Brunell, A. Nadji, and L. Nadolski, "Refined tracking procedure for the SOLEIL energy acceptance calculation," in *Proc. PAC 2003*, pp. 896–898, 2003.
- [8] H. Wiedemann, *Particle Accelerator Physics*, vol. 1. Springer, 2 ed., 2003.
- [9] J. Beringer and others (Particle Data Group), "Review of Particle Physics," *Phys. Rev. D*, vol. 86, 2012. Section 30.4.2.
- [10] Y.-S. Tsai, "Pair production and bremsstrahlung of charged leptons," *Rev. Mod. Phys.*, vol. 46, pp. 815–851, Oct 1974.
- [11] A. Xiao and M. Borland, "Monte carlo simulation of touschek effect," *Phys. Rev. ST Accel. Beams*, vol. 13, p. 074201, Jul 2010.
- [12] M. Borland *et al.*, "Lower Emittance Lattice for the Advanced Photon Source Upgrade Using Reverse Bending Magnets," in *NAPAC 2016*, pp. 877–880, 2016.
- [13] L. Farvacque, N. Carmignani, J. Chavanne, A. Franchi, G. L. Bec, S. Liuzzo, B. Nash, T. Perron, and P. Raimondi, "A Low-emittance Lattice for the ESRF," in *Proc. 2013 IPAC*, p. 79, 2013.
- [14] J. Delahaye and J. P. Potier, "Reverse bending magnets in a combined-function lattice for the CLIC damping ring," in *Proc. PAC89*, pp. 1611–1613, 1990.
- [15] A. Streun, "The anti-bend cell for ultralow emittance storage ring lattices," *NIM A*, vol. 737, pp. 148–154, 2014.
- [16] J. Carter *et al.*, "Progress on the final design of the APS Upgrade storage ring vacuum system," in *Proc. MEDSI 2018*, pp. 30–32, 2018.
- [17] V. Sajaev and M. Borland, "Commissioning Simulations for the APS Upgrade Lattice," in *Proc. IPAC15*, pp. 553–555, 2015.
- [18] V. Sajaev, "Commissioning Simulations for the APS Upgrade Lattice," *Phys. Rev. Accel. Beams*, vol. 22, p. 040102, 2019.